

Sensing adsorption kinetics through slip velocity measurements of polymer melts

Marceau Hénot,¹ Eric Drockenmuller,² Liliane Léger,¹ and Frédéric Restagno^{1,*}

¹*Laboratoire de Physique des Solides, CNRS, Univ. Paris-Sud,
Université Paris-Saclay, 91405 Orsay Cedex, France*

²*Univ Lyon, Université Lyon 1, CNRS, Ingénierie des Matériaux Polymères, UMR 5223, F-69003, Lyon, France*
(Dated: December 6, 2021)

The evolution over time of the non-linear slip behavior of a polydimethylsiloxane (PDMS) polymer melt on a weakly adsorbing surface made of short non-entangled PDMS chains densely end-grafted to the surface of a fused silica prism has been measured. The critical shear rate at which the melt enters the nonlinear slip regime has been shown to increase with time. The adsorption kinetics of the melt on the same surface has been determined independently using ellipsometry. We show that the evolution of slip can be explained by the slow adsorption of melt chains using the Brochard-de Gennes's model.

I. INTRODUCTION

Polymer chains are known to adsorb irreversibly on some surfaces from a melt or a solution. The conformations of adsorbed or grafted chains using neutron reflectivity has been extensively studied in particular by L. Au-vray and co-workers [1–6] using neutron reflectivity. Neutron reflectivity also allowed to study their interactions with a solution [7–9] or other soft matter systems [10]. If the adsorbed polymer chains are long enough, they can entangle with the bulk chains and thus modify the mechanical coupling between the solid surface and the liquid. Their effect on liquid polymer flows is of practical importance in many fields such as polymer assisted oil recovery [11–14], polymer extrusion [15–17], lubrication in industrial processes [18] or in biological systems [19]. Indeed, a fluid flowing near a wall at low Reynolds number can dissipate energy through its viscosity or through slip at the wall via friction of the last layer of fluid on the solid surface. The friction stress σ of the liquid on the solid wall can be described using the linear response assumption made by Navier [20] by $\sigma = kV$ where V is the slip velocity and k is the interfacial friction coefficient. The bulk friction coefficient ζ between two layers of molecules in the bulk can be estimated as $\zeta = \eta/a$, where a is a molecular size. In most cases, particularly for simple fluids, the friction at the wall is higher than between two layers of molecules $k > \zeta$ and the slip effect is completely negligible at the macroscopic scale [20–25], as viscous dissipation is more favorable. However, in the case of nanoscopic scale flow [26, 27] or in the case of complex fluids, slip can play a major role. To quantify flow with slip at the wall, the slip length b defined as the distance behind the wall where the velocity profile would extrapolate to zero is often used. In the case of simple shear flow, $b = V/\dot{\gamma}$ where $\dot{\gamma}$ is the shear rate.

Polymer melts on non-adsorbing surfaces can present much larger slip lengths, in the micrometric to millimetric range, so that the dissipation through slip could become

of the same order, or dominate, over the viscous dissipation. This was first conjectured by de Gennes [28]: he assumed that the interfacial friction of a linear polymer melt on a surface was similar to that of a simple fluid made of the same monomer, just because the same entities, monomers were indeed what was sliding on the surface, in both cases. As a consequence, a slip length proportional to the melt viscosity was predicted. For polymer melts submitted to shear rates in the Newtonian regime, b is thus expected to be independent of the shear rate $\dot{\gamma}$. These predictions have been well verified experimentally, especially at high enough shear rates, on some carefully prepared ideal surfaces [29–31].

Nevertheless a large number of experimental studies reported a strong dependence of b on $\dot{\gamma}$ [32–44]. For instance, the sharkskin instability that had been observed since the 40s in extrusion processes was explained by a stick slip effect resulting from nonlinear friction at the wall [15, 17, 45, 46]. This strong non-linearity has been attributed to the presence of adsorbed chains on the surfaces that can entangle with the melt [47–51] and undergo an entangled-desentangled transition when stretched under the effect of the local friction forces. The model de-

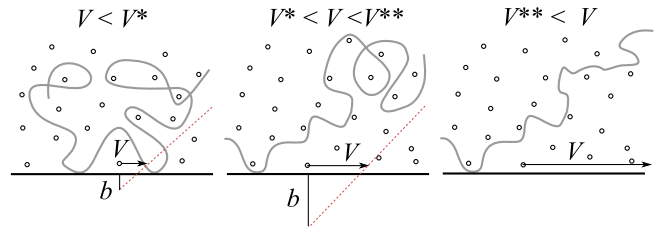


FIG. 1. Schematics of the behavior of an adsorbed polymer chain when the melt is flowing. For slip velocity below V^* the adsorbed chain is fully entangled with the melt leading to linear friction while when $V^* < V < V^{**}$ the tail is stretched and only the head of the chain is relaxed and entangled. This last regime is called marginal. For $V > V^{**}$, the adsorbed chain is completely stretched and fully disentangled from the melt. The friction is then low and linear.

veloped by Brochard *et al.* [47–50] in order to describe the effect on slip of chains end attached to the walls is illus-

* Corresponding author: frederic.restagno@u-psud.fr

trated in Figure 1. For a low enough slip velocity V , the attached chains are fully entangled with the melt, leading to high linear friction and small slip length. When V reaches a critical value V^* , the attached chains start to stretch near their attachment point while their tails remain relaxed. The size of the relaxed part diminishes when the slip velocity increases leading to a progressive reduction of the number of entanglements and thus to nonlinear friction. In this regime, called the marginal regime, the shear rate stays constant at a value $\dot{\gamma}^*$. The shear stress is thus:

$$\sigma^* = \eta \dot{\gamma}^* = \nu \frac{kT}{D_e} \quad (1)$$

where ν is the number of end attached chains per surface area, η is the viscosity of the melt and D_e is the diameter of the Edward tube [52]. At some sliding velocity value, the attached chains fully disentangle from the melt and the regime of ideal friction described by de Gennes is recovered. These three regimes were studied experimentally in detail by Migler, Massey and Durliat [35, 39–41] for adsorbed and chemically end grafted chains. In all these previous experiments, the grafted or adsorbed layer was prepared in such a way that it was not evolving with time.

The aim of the present article is to use fluid-solid friction as a probe of the adsorption kinetic of a polymer melt on a weakly adsorbing surface. To do so, we characterized the slip behavior of a melt as a function of the melt-surface contact time in the regime where the adsorbed chains have a strong influence on the slip effect, i.e. in the marginal regime.

II. EXPERIMENTS

The polymer fluid used was a silanol terminated PDMS melt with number average molar mass $M_n = 435 \text{ kg} \cdot \text{mol}^{-1}$ and a dispersity $\mathcal{D} = 1.05$, obtained by controlled fractionation of a commercial batch (Rhône-Poulenc 48V175000). The number of monomers per chain is of the order of $P \sim 5900$. For PDMS, the number of monomers within one persistence length is typically 5, hence the radius of gyration is of order 25 nm. This melt was mixed with 0.5 % by weight of fluorescently labeled photobleachable PDMS chains with a number average molar mass $M_n^* = 120 \text{ kg} \cdot \text{mol}^{-1}$ and $\mathcal{D} = 1.17$ ($P^* \sim 1600$). The fluorescent chains were lab-synthesized and labeled at both ends with nitrobenzoxadiazole groups (NBD) emitting at 550 nm [53, 54] when excited at 458 nm.

The weakly adsorbing surface where the slip was measured was the polished surface of a fused silica prism, covered with end grafted short PDMS chains with an average molar mass $2 \text{ kg} \cdot \text{mol}^{-1}$ ($N \sim 27$ monomers per chain), well below the average molar mass between entanglements, $M_e \approx 10 \text{ kg} \cdot \text{mol}^{-1}$ for PDMS [53, 55]. The synthesis protocol of these end-functionalized chains

along with the grafting procedure are detailed in Marzolin *et al.* [56]. The dry thickness of the grafted layer was $z^* = 3.2 \text{ nm}$ which corresponds to a grafting density of 10^{18} m^{-2} , i.e. 1 nm^{-2} . The dry thickness z^* is higher than the Gaussian radius of gyration ($\sim 2 \text{ nm}$) but smaller than the fully stretched length ($\sim 14 \text{ nm}$). This corresponds to the brush regime. The advancing contact angle of water of this surface was $\theta_a = 112^\circ$ with an hysteresis of 5° . The adsorption of the melt on the grafted layers was measured by rinsing the surface with toluene in a bath under agitation during 24 h. The surfaces were then dried under vacuum and the thicknesses of the remaining adsorbed layers of PDMS were measured by ellipsometry (Accurion EP3).

Slip was measured using an experimental setup previously described in Hénót *et al.* [57] relying on the analysis of the evolution under shear of the z-integrated fluorescence intensity of a pattern drawn in the sample using photobleaching. The principle of the method is illustrated in Figure 2a. The polymer melt is sandwiched between a fixed silica prism whose surface has been covered with a grafted layer of PDMS and a bare silica plate on the top. The distance h between the plates is set by nickel spacers of thickness $10 \text{ } \mu\text{m}$. The top plate can be displaced at a constant velocity V_{shear} over a distance d_{shear} using a stepped motor which induces a simple shear in the liquid. The distance d_{shear} is measured precisely using a linear variable differential transformer sensor. A laser spot at $\lambda = 458 \text{ nm}$ (Innova 90C) illuminates the sample while a home-made microscope images the fluorescence from the top. Two modes of illumination of the sample by the laser beam are available. The reading mode corresponds to a beam diameter of 2 mm when it reaches the sample. In this mode, the fluorescence can be imaged on an area of $1.5 \times 2.2 \text{ mm}$. The writing mode is obtained by placing a lens of focal length 10 cm just before the prism, which focuses the beam into the liquid. In this mode, the beam diameter is around $20 - 30 \text{ } \mu\text{m}$ inside the liquid. This focused beam is used to photobleach a pattern in the fluorescent liquid by illuminating it during 800 ms with a 20 mW incident power. Images of the fluorescence, taken before and after shear are integrated over the y axis, perpendicular to the direction of the shear, in order to obtain fluorescence intensity profiles. The Gaussian profile of Eq. 2 is fitted on the initial profile in order to determine the values of the parameters I_0 , A and σ_0 .

$$I_i(x) = I_0 - A \exp\left(-\frac{x^2}{2\sigma_0^2}\right) \quad (2)$$

The profile of Eq. 3 is then fitted on the sheared profile which gives the value of the slip distance on the bottom surface d [57]:

$$I_s(x) = I_0 - B \left[\text{erf}\left(\frac{x-d}{\sqrt{2}\sigma_0}\right) - \text{erf}\left(\frac{x-d_{\text{shear}}}{\sqrt{2}\sigma_0}\right) \right] \quad (3)$$

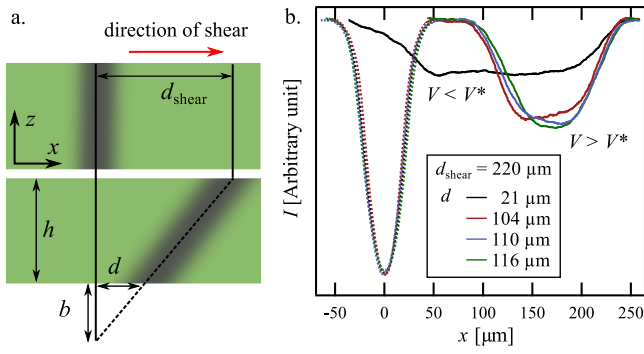


FIG. 2. a. Principle of velocimetry using photobleaching. Top: schematics of the photobleached line inside the fluid. Bottom: the liquid has been sheared over a distance d_{shear} , with a no slip boundary condition at the top plate while it has slipped at the bottom plate over a distance d which corresponds to a slip length b . The black curves represent the corresponding intensity profiles integrated over z . b. Intensity profile of the photobleached pattern before (dotted line) and after shear (plain line) for different slip velocities below and above V^* . The top plate velocity goes from 425 to 965 $\mu\text{m} \cdot \text{s}^{-1}$.

with:

$$B = \frac{A\sigma_0\sqrt{\pi}}{2(d_{\text{shear}} - d)}$$

It was checked that the slip that can occur on the top plate is negligible compared to d and d_{shear} . This is due to the strong adsorption of PDMS on this bare silica surface.

Fluorescence intensity profiles before and after shear are shown in Figure 2b. They correspond to a total displacement of the top plate of $d_{\text{shear}} = 220 \mu\text{m}$ at velocities going from 425 to 965 $\mu\text{m} \cdot \text{s}^{-1}$. For low velocities the slip velocity V stays low, while for higher velocities, a slip effect is well visible on the profiles. The corresponding slip lengths $b = hd/(d_{\text{shear}} - d)$ as a function of the velocity of the top plate V_{shear} are shown in red in Figure 3. The slip length appears to be dependent on V_{shear} . These measurements were conducted within one hour after the melt had been put in contact with the freshly made weakly adsorbing surface. Same measurements performed after 24 h and 48 h are shown respectively in green and blue in Figure 3. A measurement after 72 h was attempted but led to fracture in the melt. As can be seen, the slip behavior evolves with time. The top plate velocity required to reach a given slip length increases with time.

III. DISCUSSION

The fact that the slip behavior of the melt depends on V_{shear} means that the friction of the liquid on the surface is non-linear. Figure 4 represents the slip length as a function of the shear rate experienced by the fluid

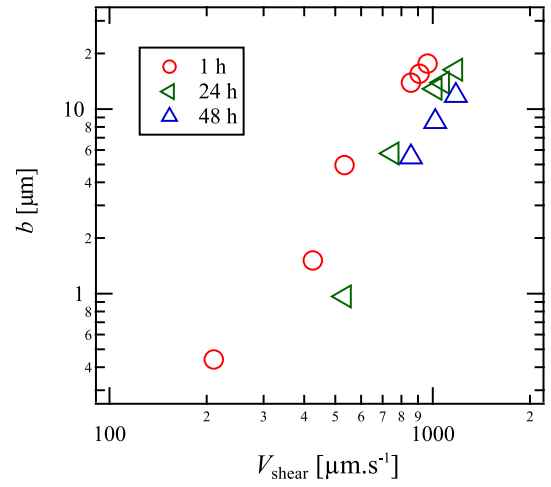


FIG. 3. Slip length as a function of V_{shear} the velocity of the top plate for different times after the melt has been put in contact with the grafted layer of PDMS.

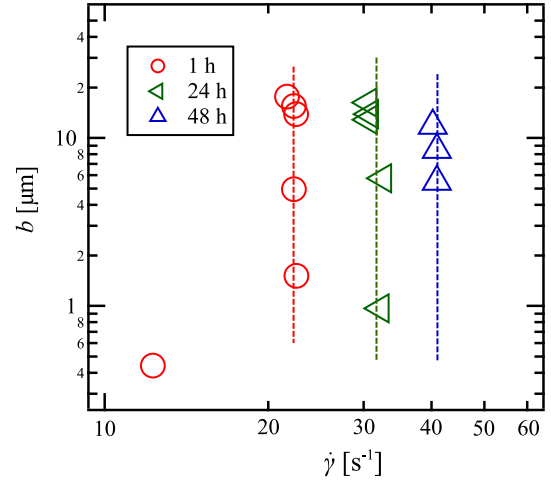


FIG. 4. Slip length as a function of the shear rate experienced by the fluid for different times after the melt has been put in contact with the grafted layer of PDMS.

$\dot{\gamma} = (V_{\text{shear}} - V)/h$. The absolute uncertainty on the determination of $\dot{\gamma}$ is dominated by the uncertainty on the distance between the two plates which is close to 10 %. However the relative uncertainty between the measurements is of the order of 0.5 s^{-1} which allows one to compare them. For each time of contact, we see a regime where the slip length evolves with V_{shear} , while the shear rate remains constant. This is characteristic of the so-called marginal regime described by Equ 1 in Brochard-de Gennes's model. The point around 12 s^{-1} after 1 h of contact thus corresponds to the fully entangled regime ($V < V^*$).

Similar weakly adsorbing Short PDMS grafted surfaces were prepared on silicon wafers, and used as tests surfaces on which the melt was deposited. These samples were kept at ambient temperature during a variable du-

ration and then rinsed thoroughly with toluene and dried under vacuum. The dry thickness h of the remaining layer of adsorbed chains was measured by ellipsometry. The same experiment was also conducted on bare silicon wafers. The results are shown in Figure 5. As expected

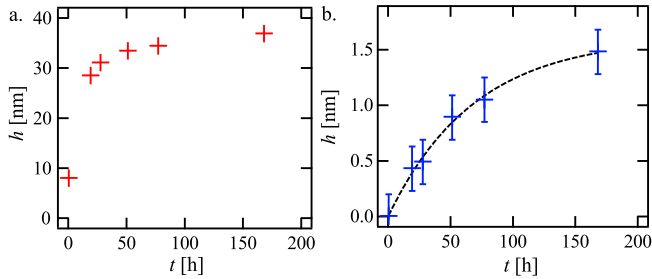


FIG. 5. Thickness of the dry layer of PDMS remaining on a bare silicon wafer (a) and on the grafted layer (b) after rinsing as a function of the duration of the contact between the melt and the surface at room temperature. The back dashed curve is an exponential adjustment of the data.

the adsorption is strong and rapid on bare silicon wafers. This is quite different from what happens on the surface covered by a protecting layer of short grafted chains, where the free chains slowly adsorb at ambient temperature. The density of adsorbed chains is related to the dry thickness h by:

$$\nu = h \frac{\rho N_A}{M_n} \quad (4)$$

Where $\rho = 965 \text{ kg} \cdot \text{m}^{-3}$ is the density of the PDMS and N_A is the Avogadro number. To be more precise, the maximum adsorption on the weakly adsorbing surface is twenty times lower than that on bare silicon wafer (i.e. 1.5 and 35 nm respectively). Indeed, in order to reach the underlying silicon oxide surface, the free chain have to stretch the relatively densely grafted short chains which induces an entropy cost. However the grafted chains are short and the melt chains do adsorb, overcoming the entropy penalty or adsorbing in holes of the grafted layer. This leads to thin but measurable adsorbed layers which still have a strong effect on the slip behavior. The maximum density for the long adsorbed chains on the grafted layer is around 10^{15} m^{-2} meaning that the molecules are separated by at least 30 nm. This is comparable to the radius of gyration. Hence, the adsorption is in the mushroom regime.

The shear rate experienced by the fluid stays constant in the marginal regime. This is consistent with early experiments done by Migler *et al.* [35] and Massey *et al.* [41] with PDMS melts having higher molar masses ($M > 610 \text{ kg} \cdot \text{mol}^{-1}$) and corresponds well to the theoretically predicted behavior. The shift with time in $\dot{\gamma}^*$ observed in Figure 4 can be interpreted in terms of an increase of the number of adsorbed chains, and related to the evolution of the dry thickness of the adsorbed layer. Rheological measurements performed on the melt (see

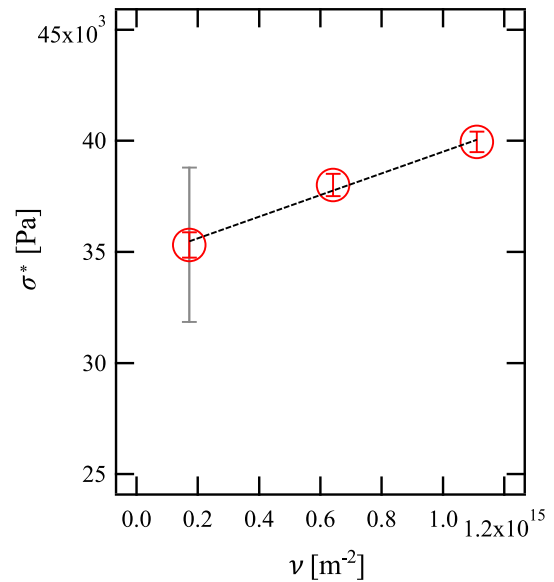


FIG. 6. Product of the critical shear rate in the marginal regime and the melt viscosity at this shear rate as a function of the density of adsorbed chains. The red error bars represent the relative uncertainty between the measurements while the gray error bar represents the absolute error. The dashed black line is a linear fit.

supplementary materials) showed that the viscosity of the melt starts to drop around 0.1 s^{-1} due to shear thinning effect. In order to take this shear thinning into account, σ^* was plotted in Figure 6 as a function of ν interpolated from the measurements of Figure 5 and using Eq 4. The relationship between these two quantities is of the form $\sigma^* = A \times \nu + \sigma_0^*$ with $A = 4.9 \pm 0.7 \times 10^{-12} \text{ N}$ and $\sigma_0^* = 35 \text{ kPa}$. Both the slope and the intercept at origin need be discussed.

Let us start by discussing the slope A . The Brochard model allows one to estimate this slope in the case of end grafted chains with no other attachment point to the surface than the grafted extremity. The value of $D_e = 2.6 \text{ nm}$ was estimated for PDMS by Ajdari *et al.* [48]. Using Eq. 1, this leads to $A_{th} \approx 1.5 \times 10^{-12} \text{ N}$. The order of magnitude is quite close to what we have obtained, but we need to account for the factor three of difference. In fact, the situation of adsorbed chains is more complex than that of end grafted chains, as adsorption on the surface can take place through any monomer. Long chains can thus entangle with the melt through any large enough tail and loop (larger than D_e). This means that the onset of marginal regime should be related to a renormalized surface density $\nu' = \alpha \nu$ with α larger than one. A loop is expected to contribute as much as two tails for symmetry reasons: each half-loop exert a force toward the adsorption point and the tension should be zero between the two. Comparing our result to eq. 1 we find $\alpha = 3$. This seems plausible and means that loops also contribute to the slip transition.

The value of the shear stress in the zero adsorption

limit σ_0^* is more puzzling: it appears to be much larger than the contribution of the adsorbed chains. For each adsorption density, there are two contributions to the friction stress: one from the adsorbed chains entangled with the melt, and one from the monomeric friction of the melt on the short chains grafted layer (with no entanglements). A first estimate for this latter contribution can be obtained writing $\sigma_0(V) = kV$ where k is the interfacial friction coefficient associated to monomer-monomer friction [28]. At the onset of the marginal regime, the slip velocity is of the order of $V^* = 40 \mu\text{m} \cdot \text{s}^{-1}$. We have previously measured the interfacial friction coefficient for a PDMS melt sliding on grafted PDMS layers at high enough sliding velocities, so that melt and grafted chains were fully disentangled. We obtained $k \approx 1 \times 10^8 \text{ kg} \cdot \text{m}^{-1} \cdot \text{s}^{-1}$ [31]. This gives a contribution to the shear stress of order of 4 kPa at the onset of the marginal regime, much too small to explain the measured B value. Such a large value of B is unexpected, and quite puzzling to explain. A possible explanation could be that the melt penetrates the layer of short grafted chains. The increasing number of monomers pertaining to grafted chains around a free chains would leads to an enhanced interfacial monomeric friction compared to large velocities situation where k has been measured. Such a penetration is certainly not total, as it would lead to higher adsorbed densities (we find weak adsorption densities, in the mushroom regime). Penetration however does exist, at least at rest, otherwise there would be no adsorption. To push further this argument and make it quantitative, more information on the degree of

penetration of the melt inside the grafted layer, and also on the role of the slip velocity on this degree of interpenetration would be needed. Such information could be obtained through neutrons reflectivity techniques for example, but the small thicknesses involved make this task delicate.

IV. CONCLUSION

We measured the evolution over time of the non-linear slip behavior of a PDMS melt using a velocimetry technique based on photobleaching on a weakly adsorbing surface made of short non-entangled PDMS chains densely end-grafted to the surface of a fused silica prism. By comparing the evolution of the critical shear rate at which the slip transition started, which increased with time, to the independently measured adsorption kinetics of the melt on the same surface, using a model developed by Brochard *et al.* [50], we showed that this effect is controlled by the slow adsorption of the chains and we extracted an average number of entangled loops and tails per adsorbed chains. We found a stress at zero adsorbed density, that we interpreted as monomeric friction of the melt on the grafted layer, higher than expected.

V. ACKNOWLEDGMENTS

This work was supported by ANR-ENCORE program (ANR-15-CE06-005). We thank I. Antoniuk for technical help.

-
- [1] Auvray, L. and De Gennes, P. G. (1986) Neutron scattering by adsorbed polymer layers. *EPL (Europhysics Letters)*, **2**(8), 647 doi: 10.1209/0295-5075/2/8/012.
 - [2] Auroy, P., Auvray, L., and Léger, L. (1990) The study of grafted polymer layers by neutron scattering. *Journal of Physics: Condensed Matter*, **2**, SA317 doi: 10.1088/0953-8984/2/S/059.
 - [3] Auroy, P., Auvray, L., and Léger, L. (1991) Characterization of the Brush Regime for Grafted Polymer Layers at the Solid-Liquid Interface. *Physical review letters*, **66**(6), 719 doi: 10.1103/PhysRevLett.66.719.
 - [4] Auroy, P., Auvray, L., and Léger, L. (1991) Structures of end-grafted polymer layers: a small-angle neutron scattering study. *Macromolecules*, **24**(9), 2523–2528 doi: 10.1021/ma00009a060.
 - [5] Auroy, P., Mir, Y., and Auvray, L. (1992) Local structure and density profile of polymer brushes. *Physical review letters*, **69**(1), 93 doi: 10.1103/PhysRevLett.69.93.
 - [6] Mir, Y., Auroy, P., and Auvray, L. (1995) Density profile of polyelectrolyte brushes. *Physical review letters*, **75**(15), 2863 doi: 10.1103/PhysRevLett.75.2863.
 - [7] Auroy, P. and Auvray, L. (1992) Collapse-stretching transition for polymer brushes: Preferential solvation. *Macromolecules*, **25**(16), 4134–4141 doi: 10.1021/ma00042a014.
 - [8] Auvray, L., Auroy, P., and Cruz, M. (1992) Structure of polymer layers adsorbed from concentrated solutions. *Journal de Physique I*, **2**(6), 943–954 doi: 10.1051/jp1:1992106.
 - [9] Auvray, L., Cruz, M., and Auroy, P. (1992) Irreversible adsorption from concentrated polymer solutions. *Journal de Physique II*, **2**(5), 1133–1140 doi: 10.1051/jp2:1992191.
 - [10] Lal, J. and Auvray, L. (1994) Perturbations of microemulsion droplets by confinement and adsorption of polymer. *Journal de Physique II*, **4**(12), 2119–2125 doi: 10.1051/jp2:1994250.
 - [11] De Vargas, L. and Manero, O. (1989) On the slip phenomenon of polymeric solutions through capillaries. *Polymer Engineering & Science*, **29**(18), 1232–1236 doi: 10.1002/pen.760291804.
 - [12] Chauveteau, G. and Zaitoun, A. (1981) Basic rheological behavior of xanthan polysaccharide solutions in porous media: Effect of pore size and polymer concentration. In *Proceedings of the First European Symposium on Enhanced Oil Recovery, Bournemouth, England, Society of Petroleum Engineers, Richardson, TX* pp. 197–212.
 - [13] Cuenca, A. and Bodiguel, H. (2012) Fluorescence photobleaching to evaluate flow velocity and hydrodynamic dispersion in nanoslits. *Lab on a Chip*, **12**(9), 1672 doi: 10.1039/c2lc21232c.

- [14] Cuenca, A. and Bodiguel, H. (2013) Submicron Flow of Polymer Solutions: Slippage Reduction due to Confinement. *Physical Review Letters*, **110**(10), 108304 doi: 10.1103/PhysRevLett.110.108304.
- [15] Ramamurthy, A. V. (1986) Wall Slip in Viscous Fluids and Influence of Materials of Construction. *Journal of Rheology*, **30**(2), 337–357 doi: 10.1122/1.549852.
- [16] Piau, J. M. and El Kissi, N. (1994) Measurement and modelling of friction in polymer melts during macroscopic slip at the wall. *Journal of non-newtonian fluid mechanics*, **54**, 121–142 doi: 10.1016/0377-0257(94)80018-9.
- [17] Denn, M. M. (2001) Extrusion instabilities and wall slip. *Annual Review of Fluid Mechanics*, **33**(1), 265–287 doi: 10.1146/annurev.fluid.33.1.265.
- [18] Cayer-Barrioz, J., Mazuyer, D., Tonck, A., and Yamaguchi, E. (2008) Drainage of a Wetting Liquid: Effective Slippage or Polymer Depletion?. *Tribology Letters*, **32**(2), 81–90 doi: 10.1007/s11249-008-9365-7.
- [19] Dédinaite, A. (2012) Biomimetic lubrication. *Soft Matter*, **8**(2), 273–284 doi: 10.1039/C1SM06335A.
- [20] Navier, C. L. Mémoire sur les lois du mouvement des fluides pp. 389–440 Imprimerie royale (1823).
- [21] Churaev, N. V., Sobolev, V. D., and Somov, A. N. (1984) Slippage of liquids over lyophobic solid surfaces. *Journal of Colloid and Interface Science*, **97**(2), 574–581 doi: 10.1016/0021-9797(84)90330-8.
- [22] Pit, R., Hervet, H., and Léger, L. (2000) Direct experimental evidence of slip in hexadecane: solid interfaces. *Physical Review Letters*, **85**(5), 980–983 doi: 10.1103/PhysRevLett.85.980.
- [23] Craig, V. S. J., Neto, C., and Williams, D. R. M. (2001) Shear-Dependent Boundary Slip in an Aqueous Newtonian Liquid. *Physical Review Letters*, **87**(5), 0545041–4 doi: 10.1103/PhysRevLett.87.054504.
- [24] Schmatko, T., Hervet, H., and Léger, L. (2005) Friction and Slip at Simple Fluid-Solid Interfaces: The Roles of the Molecular Shape and the Solid-Liquid Interaction. *Physical Review Letters*, **94**(24) doi: 10.1103/PhysRevLett.94.244501.
- [25] Neto, C., Evans, D. R., Bonaccorso, E., Butt, H., and Craig, V. S. J. (2005) Boundary slip in Newtonian liquids: a review of experimental studies. *Reports on Progress in Physics*, **68**(12), 2859–2897 doi: 10.1088/0034-4885/68/12/R05.
- [26] Cottin-Bizonne, C., Jurine, S., Baudry, J., Crassous, J., Restagno, F., and Charlaix, E. (2002) Nanorheology: an Investigation of the Boundary Condition at Hydrophobic and Hydrophilic Interfaces. *The European Physical Journal E*, **9**(1), 47–53 doi: 10.1140/epje/i2001-10112-9.
- [27] Secchi, E., Marbach, S., Niguès, A., Stein, D., Siria, A., and Bocquet, L. (2016) Massive radius-dependent flow slippage in carbon nanotubes. *Nature*, **537**(7619), 210–213 doi: 10.1038/nature19315.
- [28] De Gennes, P. G. (1979) Ecoulements viscométriques de polymères enchevêtrés. *C. R. Acad. Sc. Paris*, pp. 219–220 doi: 10.1142/9789812564849_0019.
- [29] Wang, S.-Q. and Drda, P. P. (1997) Molecular instabilities in capillary flow of polymer melts: interfacial stick-slip transition, wall slip and extrudate distortion. *Macromol. Chem. Phys.*, **198**, 673–701 doi: 10.1002/macp.1997.021980302.
- [30] Bäumchen, O., Fetzer, R., and Jacobs, K. (2009) Reduced Interfacial Entanglement Density Affects the Boundary Conditions of Polymer Flow. *Physical Review Letters*, **103**(24) doi: 10.1103/PhysRevLett.103.247801.
- [31] Hénot, M., Drockenmüller, E., Léger, L., and Restagno, F. (2018) Friction of Polymers: from PDMS Melts to PDMS Elastomers. *ACS Macro Letters*, **7**(1), 112–115 doi: 10.1021/acsmacrolett.7b00842.
- [32] Lim, F. J. and Schowalter, W. R. (1989) Wall Slip of Narrow Molecular Weight Distribution Polybutadienes. *Journal of Rheology*, **33**(8), 1359–1382 doi: 10.1122/1.550073.
- [33] Kissi, N. E. and Piau, J. (1990) The different capillary flow regimes of entangled polydimethylsiloxane polymers: macroscopic slip at the wall, hysteresis and cork flow. *Journal of Non-Newtonian Fluid Mechanics*, **37**(1), 55–94 doi: 10.1016/0377-0257(90)80004-J.
- [34] Hatzikiriakos, S. G. and Dealy, J. M. (1992) Wall slip of molten high density polyethylenes. II. Capillary rheometer studies. *Journal of Rheology*, **36**(4), 703–741 doi: 10.1122/1.550313.
- [35] Migler, K. B., Hervet, H., and Léger, L. (1993) Slip transition of a polymer melt under shear-stress. *Physical Review Letters*, **70**(3), 287–290 doi: 10.1103/PhysRevLett.70.287.
- [36] Drda, P. P. and Wang, S.-Q. (oct, 1995) Stick-Slip Transition at Polymer Melt/Solid Interfaces. *Physical Review Letters*, **75**, 2698–2701 doi: 10.1103/PhysRevLett.75.2698.
- [37] Wang, S.-Q. and Drda, P. A. (1996) Superfluid-Like Stick-Slip Transition in Capillary Flow of Linear Polyethylene Melts. 1. General Features. *Macromolecules*, **29**(7), 2627–2632 doi: 10.1021/ma950898q.
- [38] Wang, S.-Q. and Drda, P. A. (1996) Stick-Slip Transition in Capillary Flow of Polyethylene. 2. Molecular Weight Dependence and Low-Temperature Anomaly. *Macromolecules*, **29**(11), 4115–4119 doi: 10.1021/ma951512e.
- [39] Durliat, E., Hervet, H., and Léger, L. (1997) Influence of grafting density on wall slip of a polymer melt on a polymer brush. *Europhysics Letters*, **38**(5), 383–388 doi: 10.1209/epl/i1997-00255-3.
- [40] Léger, L., Hervet, H., Massey, G., and Durliat, E. (1997) Wall slip in polymer melts. *Journal of Physics: Condensed Matter*, **9**(37), 7719–7740 doi: 10.1088/0953-8984/9/37/006.
- [41] Massey, G., Hervet, H., and Léger, L. (1998) Investigation of the slip transition at the melt polymer interface. *Europhysics Letters (EPL)*, **43**(1), 83–88 doi: 10.1209/epl/i1998-00323-8.
- [42] Chennevière, A., Cousin, F., Boué, F., Drockenmüller, E., Shull, K. R., Léger, L., and Restagno, F. (2016) Direct Molecular Evidence of the Origin of Slip of Polymer Melts on Grafted Brushes. *Macromolecules*, **49**(6), 2348–2353 doi: 10.1021/acs.macromol.5b02505.
- [43] Ilton, M., Salez, T., Fowler, P. D., Rivetti, M., Aly, M., Benzaquen, M., McGraw, J. D., Raphaël, E., Dalnoki-Veress, K., and Bäumchen, O. (2017) Beyond the Navier-de Gennes Paradigm: Slip Inhibition on Ideal Substrates. *arXiv preprint arXiv:1708.03420*, arXiv: 1708.03420.
- [44] Gay, C. (1999) New concepts for the slippage of an entangled polymer melt at a grafted solid interface. *The European Physical Journal B - Condensed Matter and Complex Systems*, **7**(2), 251–262.
- [45] Rielly, F. J. and Price, W. L. (1961) Plastic flow in injection molds. *SPE J.*, pp. 1097–101.
- [46] Kalika, D. S. and Denn, M. M. (1987) Wall Slip and Extrudate Distortion in Linear Low Density

- Polyethylene. *Journal of Rheology*, **31**(8), 815–834 doi: 10.1122/1.549942.
- [47] Brochard, F. and De Gennes, P. G. (1992) Shear-dependent slippage at a polymer/solid interface. *Langmuir*, **8**(12), 3033–3037 doi: 10.1021/la00048a030.
- [48] Adjari, A., Brochard-Wyart, F., de Gennes, P.-G., Leibler, L., Viovy, J.-L., and Rubinstein, M. (1994) Slippage of an entangled polymer melt on a grafted surface. *Physica A: Statistical Mechanics and its Applications*, **204**(1), 17–39 doi: 10.1016/0378-4371(94)90415-4.
- [49] Ajdari, A., Brochard-Wyart, F., Gay, C., and De Gennes, P. G. (1995) Drag on a Tethered Chain Moving in a Polymer Melt. *Journal de Physique II*, **5**(4), 491 doi: 10.1051/jp2:1995145.
- [50] Brochard-Wyart, F., Gay, C., and de Gennes, P. G. (1996) Slippage of Polymer Melts on Grafted Surfaces. *Macromolecules*, **29**(1), 377–382 doi: 10.1021/ma950753j.
- [51] Jeong, S., Cho, S., Kim, J. M., and Baig, C. (2017) Molecular mechanisms of interfacial slip for polymer melts under shear flow. *Journal of Rheology*, **61**(2), 253–264 doi: 10.1122/1.4974907.
- [52] De Gennes, P. (1979) *Scaling Concepts in Polymer Physics*, Cornell University Press, .
- [53] Léger, L., Hervet, H., Auroy, P., Boucher, E., and Massey, G. (1996) The reptation model: tests through diffusion measurements in linear polymer melts. In Piau, J.-M. and Agassant, J.-F., (eds.), *Rheology for Polymer Melt Processing*, Vol. 5 of Rheology Series, pp. 1–16 Elsevier doi: 10.1016/S0169-3107(96)80002-5.
- [54] Cohen, C., Damiron, D., Dkhil, S. B., Drockenmuller, E., Restagno, F., and Léger, L. (2012) Synthesis of well-defined poly(dimethylsiloxane) telechelics having nitrobenzoxadiazole fluorescent chain-ends via thiol-ene coupling. *Journal of Polymer Science Part A: Polymer Chemistry*, **50**(9), 1827–1833 doi: 10.1002/pola.25952.
- [55] Fetters, L. J., Lohse, D. J., Richter, D., Witten, T. A., and Zirkel, A. (1994) Connection between Polymer Molecular Weight, Density, Chain Dimensions, and Melt Viscoelastic Properties. *Macromolecules*, **27**(17), 4639–4647 doi: 10.1021/ma00095a001.
- [56] Marzolin, C., Auroy, P., Deruelle, M., Folkers, J. P., Léger, L., and Menelle, A. (2001) Neutron Reflectometry Study of the Segment-Density Profiles in End-Grafted and Irreversibly Adsorbed Layers of Polymer in Good Solvents. *Macromolecules*, **34**(25), 8694–8700 doi: 10.1021/ma010156z.
- [57] Hénot, M., Chennevière, A., Drockenmuller, E., Léger, L., and Restagno, F. (2017) Comparison of the Slip of a PDMS Melt on Weakly Adsorbing Surfaces Measured by a New Photobleaching-Based Technique. *Macromolecules*, **50**(14), 5592–5598 doi: 10.1021/acs.macromol.7b00601.
- [58] Cox, W. P. and Merz, E. H. (1958) Correlation of dynamic and steady flow viscosities. *Journal of Polymer Science*, **28**(118), 619–622 doi: 10.1002/pol.1958.1202811812.
- [59] Macosko, C. W. (1994) *Rheology: Principles, Measurements, and Applications*, Wiley-VCH, .

Supplementary Materials:

Figure 7.a shows the viscosity of the 435 kg·mol⁻¹ PDMS melts used in this work as a function of the angular frequency. This measurement was performed at 20 °C under oscillatory flow using a cone-plate geometry on an Anton Paar MCR302 rheometer. The relation between the viscosity obtained using oscillatory flow η^* and the viscosity under shear flow η is given by the Cox-Merz [58, 59] rule $\eta^*(\omega) = \eta(\dot{\gamma})$. The shear stress $\sigma = \eta\dot{\gamma}$ is plotted in Figure 7.b as a function of the shear rate.

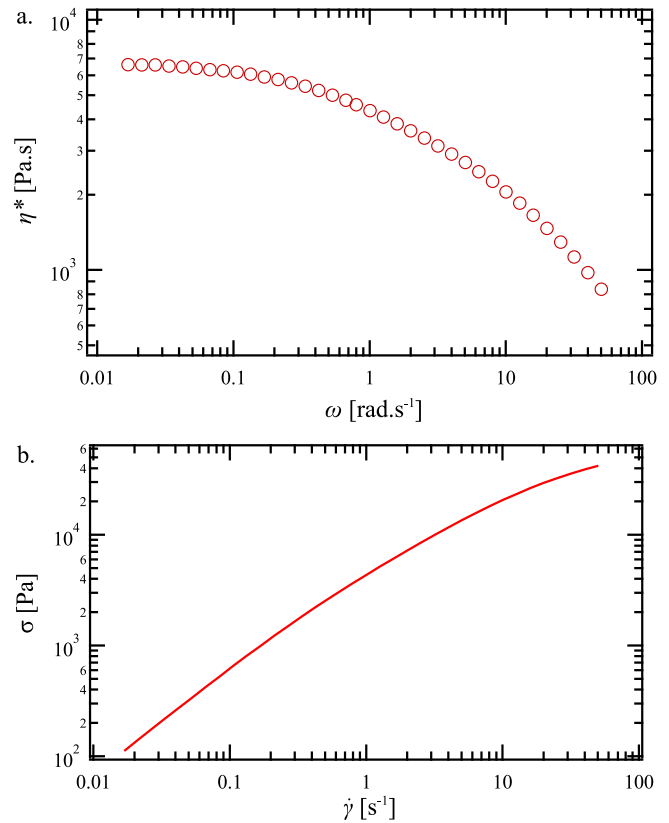


FIG. 7. a. Viscosity at 20 °C of a 435 kg·mol⁻¹ PDMS melt as a function of the angular frequency. The data were measured under oscillations using a cone-plate geometry. b. Shear stress $\sigma = \eta\dot{\gamma}$ as a function of the shear rate $\dot{\gamma}$.